

## *Ab initio* optical properties of Si(100)

Maurizia Palummo, Giovanni Onida, and Rodolfo Del Sole

*Istituto Nazionale per la Fisica della Materia—Dipartimento di Fisica dell' Università di Roma Tor Vergata,  
Via della Ricerca Scientifica, I-00133 Roma, Italy*

Bernardo S. Mendoza

*Centro de Investigación en Óptica, A.C. León, Guanajuato, Mexico*

(Received 18 February 1999)

We compute the linear optical properties of different reconstructions of the clean and hydrogenated Si(100) surface within DFT-LDA, using norm-conserving pseudopotentials. The equilibrium atomic geometries of the surfaces, determined from self-consistent total-energy calculations within the Car-Parrinello scheme, strongly influence reflectance anisotropy spectra, showing differences between the  $p(2\times 2)$  and  $c(4\times 2)$  reconstructions. The differential reflectivity spectrum for the  $c(4\times 2)$  reconstruction shows a positive peak at  $\hbar\omega < 1$  eV, in agreement with experimental results. [S0163-1829(99)03928-4]

### I. INTRODUCTION

The optical spectroscopy of surfaces is becoming more and more popular as a nondestructive and versatile tool of surface analysis. At variance with electron spectroscopies, it does not require ultrahigh vacuum conditions, so that it can be used to monitor the growth of epilayers in molecular-beam epitaxy and metal-organic chemical-vapor deposition techniques. However, the full potentiality of these kinds of techniques can be exploited only by a strong interaction of experimental and theoretical work, due to the difficulty of interpreting the spectra.

The dream of theorists is to compute realistic surface optical properties for useful comparison with experiments, given only the atomic species and positions. Until now most of the calculations were based on the semiempirical tight-binding (TB) scheme, which, in spite of its successes,<sup>1</sup> is not completely satisfactory from the theoretical point of view; in fact, it is not self-consistent, and needs some experimental inputs to determine the electron bands and the optical properties. Only in the last years, due to the growing development of computational methods and computer performances, calculations of the optical properties within a first-principle approach started to appear.<sup>2-4</sup> In principle, the correct procedure should be the calculation of the electronic states in a many-body approach, including self-energy effects, and taking into account the electron-hole interaction and local-field effects to obtain the dielectric function. Actually, the state of the art is the determination of the single-particle electron states using the density-functional theory (DFT) scheme<sup>5</sup> in the local-density approximation (LDA).<sup>6</sup>

The Si(100) surface is extensively studied, both from the experimental and theoretical points of view, due to its technological importance. Now, it is generally accepted that its atomic structure is characterized by the presence of asymmetric buckled surface dimers along the  $[01\bar{1}]$  direction, which implies at least a  $(2\times 1)$  reconstruction. Two other energetically competing (favored) reconstructions are possible, within the same top-atom bonding characteristic. The alternation of dimer buckling along the  $[01\bar{1}]$  dimer rows

leads to a  $p(2\times 2)$  reconstruction, while the alternation of buckling angles also along the direction perpendicular to the rows leads to the  $c(4\times 2)$  phase.<sup>7</sup>

The actual geometry of the surface at room and low temperature is still controversial. The observed filled and empty surface states at room temperature were reasonably referred to as  $c(4\times 2)$  domains present in a  $(2\times 1)$  disordered structure.<sup>8,9</sup> Moreover a phase transition from the ordered  $c(4\times 2)$  to a disordered  $(2\times 1)$  reconstruction, with small  $c(4\times 2)$  and  $p(2\times 2)$  domains, has been observed with low-energy electron diffraction (LEED) at 200 K.<sup>10</sup> Recently Yokoyama and Takayanagi<sup>11</sup> showed with STM measurements the suppressive influence of steps on the phase transition leading to a long-range ordered  $c(4\times 2)$  structure. From *ab initio* molecular-dynamics simulations Shkrebtii *et al.*<sup>12</sup> established that the room temperature Si(100) corresponds to a mixture of the  $c(4\times 2)$  and  $p(2\times 2)$  geometries, together with instantaneous symmetriclike “twisted dimers” configurations. At room temperature scanning tunneling microscopy (STM) images show a symmetric configuration, due to the quick flipping of dimers between their two possible orientations.<sup>13</sup> Recently Shigekawa *et al.*<sup>14</sup> showed that such flipping and the appearance of symmetric dimers in STM is connected to a migrating phase defect at domain boundaries.

In recent years different experimental studies, with reflectance anisotropy spectroscopy (RAS) and surface differential reflectivity (SDR) techniques, have been performed on Si(100), both on clean and adsorbate-covered surfaces. Several theoretical calculations are available, both based on tight-binding<sup>1</sup> and first-principles,<sup>3,15,16</sup> for the  $2\times 1$  and  $2\times 2$  reconstructions, but none are available for the most stable  $c(4\times 2)$  phase. For this reason, and also for the difficulty of preparing monodomain step-free surfaces, not all features in the optical spectra are well understood. The agreement between the theoretical spectra obtained with the TB scheme and those computed within the DFT-LDA is not always satisfactory, confirming that the study of the optical properties of this surface is not a simple matter. From the experimental point of view, Shioda and van der Weide<sup>17</sup> and Jaloviar *et al.*<sup>18</sup> pointed out recently the importance of a correct preparation of the clean surface (a terrace width about 1000 times larger than that obtained on vicinal surfaces, typi-

cally of 40–160 Å, can be obtained with the techniques employed in Refs. 17 and 18) in order to minimize spurious effects due to the steps. In this way, the experiments are better suited to be compared with the theoretical results.

The purpose of this work is to produce a thorough *ab initio* calculation of the optical properties of this surface, including the ground-state  $c(4 \times 2)$  reconstruction, to be used to interpret reflectance anisotropy (RA) spectra. We also calculate the optical properties of the hydrogen-covered surface and use them to determine SDR spectra.

The paper is organized as follows: in Sec. II the theory for the calculation of the optical spectra is reviewed, in Sec. III the method of calculation is explained, and in Sec. IV the optical spectra for the various surfaces are presented and compared with the experiments. Finally, the conclusions are given in Sec. V.

## II. THEORY

The surface contribution to the reflectivity is defined as the deviation of the reflectance with respect to the Fresnel formula, which is valid for an abrupt surface. The general formulas for the reflection coefficient of  $s$  and  $p$  radiation can be found solving the light-propagating equations at surfaces, when inhomogeneity and anisotropy at the surface are fully taken into account (see Ref. 19 for a review). For normally incident light the correction to the Fresnel formula for the reflectivity is<sup>2</sup>

$$\frac{\Delta R_i(\omega)}{R_0(\omega)} = \frac{4\omega}{c} \text{Im} \frac{\Delta \epsilon_{ii}(\omega)}{\epsilon_b(\omega) - 1}, \quad (1)$$

where  $\epsilon_b$  is the bulk dielectric function,  $R_0$  is the standard Fresnel reflectivity, and the subscript  $i$  refers to the direction of light polarization.  $\Delta \epsilon_{ii}$  is directly related to the macroscopic dielectric tensor  $\epsilon_{ij}$  of a semi-infinite solid,<sup>20</sup> and is dimensionally a length. In a repeated slab geometry, introduced in order to simulate the real surface,  $\Delta \epsilon_{ii}$  is given by

$$\Delta \epsilon_{ii} = d[1 + 4\pi \alpha_{ii}^{hs} - \epsilon_b(\omega)], \quad (2)$$

where  $d$  is half of the slab thickness and  $\alpha_{ii}^{hs}$  is the half-slab polarizability. For this geometry, the change of reflectivity with respect to the Fresnel formula reduces to

$$\frac{\Delta R_i(\omega)}{R_0(\omega)} = \frac{4\omega d}{c} \text{Im} \frac{4\pi \alpha_{ii}^{hs}(\omega)}{\epsilon_b(\omega) - 1}. \quad (3)$$

The imaginary part of  $\alpha_{ii}^{hs}$  in the single-particle scheme adopted here can be related to the transition probabilities between slab eigenstates<sup>2</sup>

$$\text{Im} m[\alpha_{ii}^{hs}(\omega)] = \frac{\pi e^2}{m^2 \omega^2 A d} \sum_{\vec{k}, \nu, c} |p_{\nu, c}^i(\vec{k})|^2 \times \delta(E_c(\vec{k}) - E_\nu(\vec{k}) - \hbar\omega), \quad (4)$$

where  $p_{\nu, c}^i(\vec{k})$  denotes the matrix element of the  $i$  component of the momentum operator between valence states ( $\nu$ ) and conduction states ( $c$ ), and  $A$  is the area of the sample surface. The  $k$  space integration is written as a sum over  $\vec{k}$  vectors in the two-dimensional Brillouin zone. The real parts of the half-slab polarizability and bulk dielectric function are obtained via the Kramers-Kronig transform. In the presence

TABLE I. Calculated buckling, and dimer length, for the  $(2 \times 1)$ ,  $c(4 \times 2)$ , and  $p(2 \times 2)$  Si(100) reconstructions. In parentheses, the value obtained if the self-consistent geometry optimization is performed at an unconverged kinetic-energy cutoff (10 Ry.)

Reconstruction	Dimer buckling (Å)	Dimer length (Å)
$(2 \times 1)$	0.71(0.56)	2.27(2.34)
$c(4 \times 2)$	0.75	2.29
$p(2 \times 2)$	0.70	2.28

of a nonlocal potential, the momentum operator in Eq. (4), describing the coupling of electrons with the radiation, should be replaced by the velocity operator.<sup>21</sup> However, Pulci *et al.*<sup>4</sup> have shown that to neglect this effect has a negligible influence on the RA.

Using Eq. (3) and Eq. (4) it is then possible to compute RAS and SDR spectra. In particular, the RA measures the difference in the reflectivity, as function of photon energy, for light polarized in two orthogonal directions in the specimen surface, i.e.,

$$\frac{\Delta R}{R_0} = \frac{\Delta R_y - \Delta R_x}{R_0}. \quad (5)$$

On the other hand, SDR measures the difference of the reflectance (with unpolarized or polarized light) between the clean and the covered surface:

$$\Delta R/R = \frac{\Delta R_{\text{clean}} - \Delta R_{\text{cov}}}{R_0}. \quad (6)$$

## III. METHOD

The electronic wave functions and eigenvalues are obtained from a self-consistent calculation, in the standard DFT-LDA scheme,<sup>5</sup> using a plane-waves basis set and the Ceperley-Alder exchange-correlation potential as parametrized by Perdew and Zunger.<sup>6</sup> The electron-ion interactions are treated by norm-conserving, fully separable *ab initio* pseudopotentials,<sup>22,23</sup> and a kinetic-energy cutoff of 15 Ry is used. The crystal with its surface is simulated by a repeated slab; 12 atomic layers and a vacuum region of four empty layers are needed to obtain a good convergence of the optical spectra of Si(100). For each structure considered the atomic positions correspond to the fully relaxed configuration obtained by Car-Parrinello molecular-dynamics runs. Three different reconstructions,  $(2 \times 1)$ ,  $p(2 \times 2)$ , and  $c(4 \times 2)$ , were considered. In Table I we report the structural parameters obtained for the various reconstructions of the clean surface. In order to obtain SDR spectra, calculations were performed also for a passivated surface [two hydrogens per surface Si atom—yielding a bulklike terminated  $(1 \times 1)$  surface without any dimers], using the same ingredients as for the corresponding clean surfaces. In the calculation of the optical spectra, we verified that the use of a reduced kinetic-energy cutoff (10 Ry instead of 15 Ry) does not change the resulting spectra appreciably. The gain in computational cost was then exploited to perform very extended convergence tests with respect to the  $k$ -points sampling used. We found that for the  $(2 \times 1)$  and hydrogenated surfaces a 64  $k$ -points set is necessary and sufficient to obtain converged spectra in the range

0–5 eV, while for the  $c(4\times 2)$  and  $p(2\times 2)$  reconstructions, due to the smaller Brillouin zone (BZ), 32  $k$  points are enough. For each surface, we compute Eq. (4) using a number of empty states within 1 Ry from the conduction-band minimum.

In order to compare the theoretical spectra with the experimental curves, we apply an upward rigid shift  $\Delta = 0.5$  eV to the conduction bands (in agreement with the results of previous  $GW$  calculations<sup>7,24</sup> on this surface) due to the well-known underestimation of the gaps in the DFT-LDA method. The momentum matrix elements are renormalized with the factor  $(E_c - E_v + \Delta)/(E_c - E_v)$ , according to the recipe of Del Sole and Girlanda.<sup>25</sup>

#### IV. OPTICAL SPECTRA

We obtain band structures in good agreement with other, well-converged DFT-LDA calculations that appeared in the literature,<sup>24,26</sup> in particular with those of Ref. 23. For the  $(2\times 1)$  reconstruction, the  $\pi$  and  $\pi^*$  surface states show a rather strong dispersion along the dimer rows ( $J$ - $K$ ,  $J'$ - $\Gamma$  directions). This implies a relevant interaction between adjacent dimers in the same row, while the flatter dispersion along the dimer direction (i.e., perpendicularly to the row) indicates a small interaction of dimers belonging to different rows. The  $c(4\times 2)$  and  $p(2\times 2)$  reconstructions, in contrast with the  $(2\times 1)$  case, show two occupied and two empty dangling-bond surface bands, in agreement with angle-resolved ultraviolet photoemission spectroscopy (ARUPS) experiments.<sup>8</sup> The dispersion of the unoccupied  $\pi^*$  surface state of the  $c(4\times 2)$  reconstruction is in good agreement with recent standing-wave patterns measurements, obtained with STM at low temperature.<sup>27</sup>

In Fig. 1 we show the RA spectra obtained for the  $(2\times 1)$  surface using three different geometries: the first with symmetric dimers, the second with a buckling of 0.56 Å (similar to Kipp's calculation<sup>3</sup>), and the last of 0.71 Å (which corresponds to our fully converged geometry at the cutoff of 15 Ry). The changes in the theoretical results are evident: the first low-energy peak, essentially due to dimer surface states, shifts from 1 to 1.4 eV (due to an opening of the gaps) and changes its sign, in going from the symmetric to the asymmetric case. The same peak increases in strength and shifts slightly to higher energy (1.6 eV) with the increase of the buckling. On the other hand, the positive peak at 4.3 eV, which is always present in the experimental spectra, reduces with the increase of the buckling.

Figure 2 shows the RAS obtained for the  $c(4\times 2)$  reconstruction. Our results for the  $p(2\times 2)$  and  $(2\times 1)$  spectra are also included. The latter are consistent with the results obtained by Kipp et al.,<sup>3</sup> although not identical due to the different equilibrium geometries at which the optical spectra have been calculated. The  $c(4\times 2)$  and  $p(2\times 2)$  spectra show, however, a larger anisotropy on the low-frequency side, due to transitions across the folded dangling-bond bands, while the  $(2\times 1)$  reconstruction has a single negative peak in this range, at about 1.4 eV. Differences are present especially below  $\hbar\omega < 1.5$  eV between the  $c(4\times 2)$  and  $p(2\times 2)$  reconstructions confirming the dependence of the spectra upon the details of the reconstruction, in particular upon the ordering of the buckled dimers along and perpen-

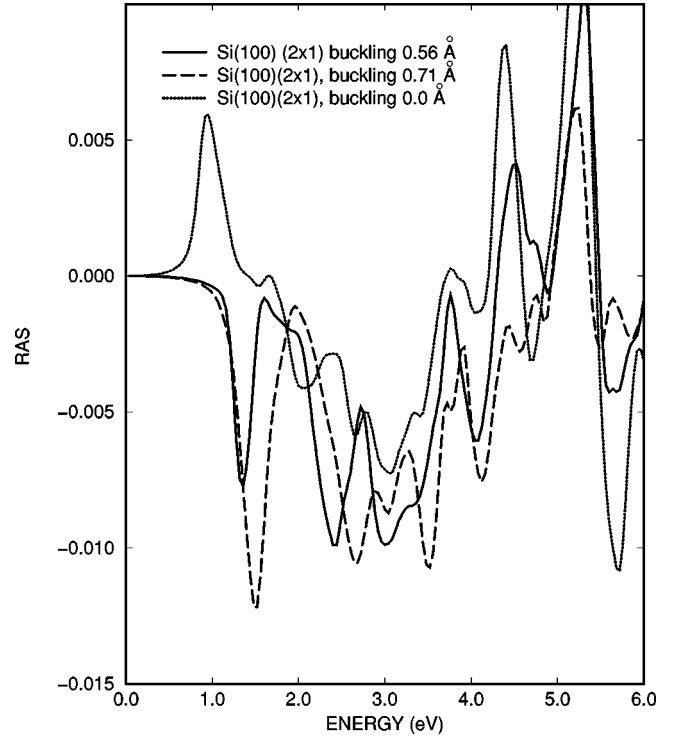


FIG. 1. Theoretical DFT-LDA RA spectra (a scissor operator of 0.5 eV is applied as discussed in the text) for the  $2\times 1$  clean surface, as a function of dimer buckling. The buckling of 0.0 Å (dotted line) corresponds to symmetric dimers. The reflectance anisotropy is defined as in Eq. (5), where  $y(x)$  is the direction parallel (perpendicular) to the dimers.

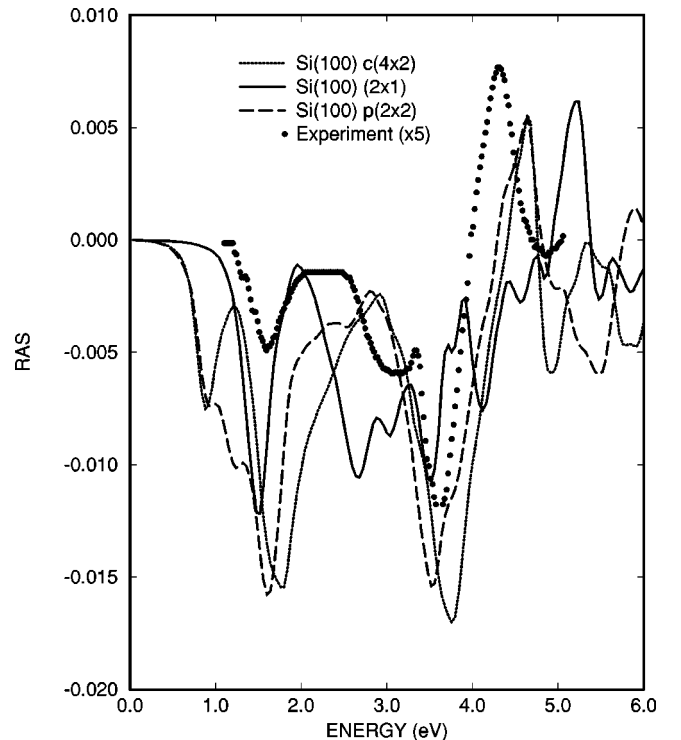


FIG. 2. RA (defined as in Fig. 1) theoretical spectra obtained with the different Si(100) reconstructions considered: full line:  $(2\times 1)$ ; dashed line:  $p(2\times 2)$ ; dotted line:  $c(4\times 2)$ . The experimental results, (Ref. 17) scaled up by a factor of 5, are also shown.

dicularly to the rows. The comparison of the overall shape with the measurements obtained by Shioda and van der Weide<sup>17</sup> is generally good, showing that the various features of the experimental spectra are due essentially to the different reconstructions present in the specimens.<sup>28</sup>

The interpretation of the experimental spectra is complicated by the disordered nature of the dimer buckling at room temperature, and by spurious effects due to the steps, or defects, that cannot be completely eliminated. The negative peak close to 3.7 eV can be explained by any of the three structures considered in Fig. 2, while the 3-eV structure implies the presence of  $(2 \times 1)$  domains at room temperature. Especially for the peak at about 4.3 eV, the comparison with the experiment is not completely clear. Cole *et al.*<sup>29</sup> found that its intensity is different in different samples, and decreases almost linearly while increasing the temperature. Shioda and van der Weide<sup>17</sup> found a similar behavior by decreasing the miscut angle of the vicinal surfaces, which corresponds to reducing the majority domain coverage (or, in other words, the anisotropy of the surface). Yasuda *et al.*,<sup>30</sup> from the analysis of their room-temperature (RT) spectra, concluded that this peak is essentially originated by a step-induced dicroism; however, the opposite conclusion has been reached by Jaloviar *et al.*,<sup>18</sup> who singled out the contribution of the steps to the RA. In our spectra a peak in the energy region around 4.3 eV is present for the  $p(2 \times 2)$  and  $c(4 \times 2)$  reconstructions, in agreement with the observed reduction with increasing temperature. On the other hand, as shown in Fig. 1, a peak at the same energy is present also in the  $(2 \times 1)$  case, and its intensity depends on the dimer buckling. Hence, we conclude, in agreement with Refs. 17 and 18, that this structure does not arise from the steps.

SDR experiments on the clean Si(100) surface for  $\hbar\omega < 1$  eV were carried out in 1983 by Chabal *et al.*<sup>31</sup> using the multiple internal total reflection arrangement. In 1980 Wierenga *et al.*,<sup>32</sup> and more recently Keim *et al.*,<sup>33</sup> measured SDR using normal-incidence external reflection. Hydrogen, oxygen, or water were used in the experiments in order to saturate the dangling bonds (only oxygen was used in the last one). In Fig. 3 we report theoretical SDR spectra calculated using, as the clean surface contribution, the  $c(4 \times 2)$ , the  $p(2 \times 2)$ , and the  $(2 \times 1)$  reconstructions, respectively. The  $(1 \times 1)$  H-covered surface is used as the reference surface. The experimental results of Refs. 31 and 32 are also shown. The positive peak at about 1.5 eV, present in the experimental spectra, is confirmed by our theoretical analysis. The first peak below 1 eV found by Chabal *et al.*<sup>31</sup> appears only when the reflectivity of the clean  $c(4 \times 2)$  reconstruction is used in Eqs. (4) and (6), although a shoulder is also present for the  $p(2 \times 2)$  reconstruction. [A peak at the same energy is visible also in electron-energy-loss spectroscopy (EELS) spectra.<sup>34</sup>] Experimentally, the intensity of this peak is found to be weakly dependent on the temperature from 40 K to room temperature. Different explanations of this structure have been proposed in the past: in EELS experiments it was interpreted as a direct transition at  $\Gamma$  from the bulk top valence to an empty surface state, while in SDR experiments it was explained as an indirect transition. Instead, in Ref. 1 it was interpreted in terms of transitions across the dangling bonds of flipping dimers, when these are instantaneously unbuckled: in this position indeed, the energy separation has

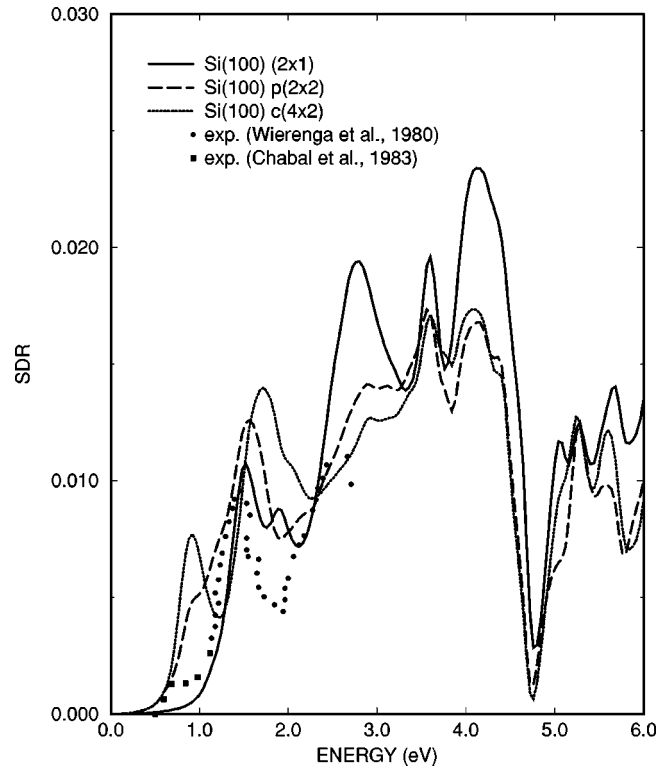


FIG. 3. SDR theoretical spectra obtained considering different reconstructions for the clean surface: full line:  $(2 \times 1)$ ; dashed line:  $p(2 \times 2)$ ; dotted line:  $c(4 \times 2)$ . The hydrogenated surface is  $(1 \times 1)$  with 2 ML of H. The experimental results from Refs. 31 and 32 are shown by squares and dots, respectively.

the right value to produce a peak just below 1 eV (see the dotted curve in Fig. 1). Although this explanation cannot be ruled out, we may now argue that the SDR structure below 1 eV could be due to the presence of  $c(4 \times 2)$  and  $p(2 \times 2)$  domains, where it is essentially due to transitions from bulk states near the top valence to unoccupied surface states. The small intensity of the experimental peak may be due to the small fraction of  $c(4 \times 2)$  domains, caused by thermal disorder as well as by the presence of defects or steps, which can suppress the long-range ordered structures.

At higher energies, a peak at about 2.5 eV is reported in Ref. 32 while two peaks at 2.90 and 3.95 eV are present in the experimental spectra of Ref. 33 when the surface is exposed to  $\text{NO}_2$ , and a further small peak appears at 3.1 eV when molecular oxygen is used. The authors of Ref. 33 argue that the peaks at 2.9 and 3.95 eV are related to transitions between surface states; instead, in our theoretical analysis for all the reconstructions studied, all spectral features above 2 eV are essentially due to surface-bulk, bulk-surface, and bulk-bulk transitions.

The agreement between our DFT-LDA RA spectra and those obtained in the TB method is limited, even if the same geometry is used. We show in Fig. 4(a) the RA calculated according to the two methods for the  $2 \times 1$  reconstruction, using a buckling of 0.56 Å (as for the full-line curve in Fig. 1), which is very close to that of Ref. 1. As previously found,<sup>3,15</sup> the sign of the RAS at about 1.5 eV, due to transitions across surface states, is the opposite of that obtained with the nearest-neighbors TB calculations. The latter coin-

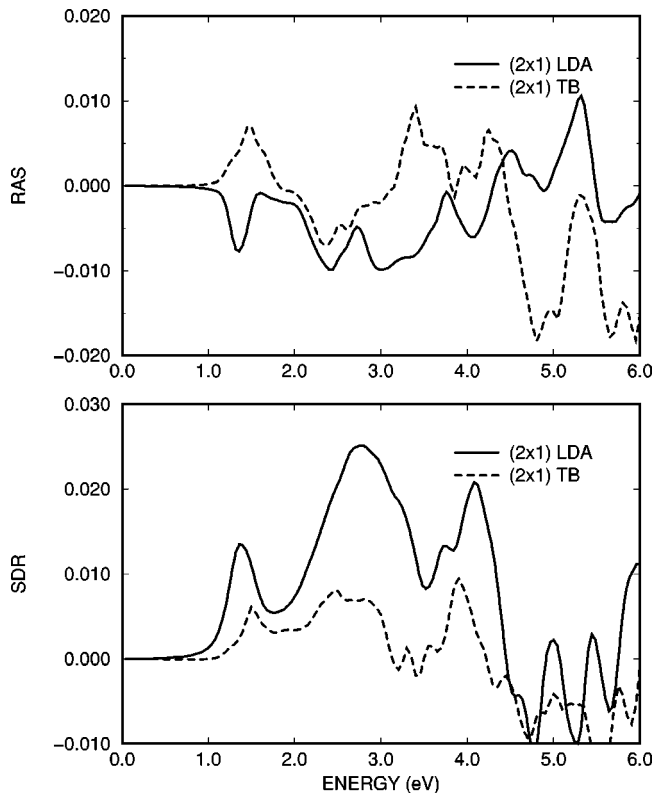


FIG. 4. Comparison of plane-wave and TB results for the (a) reflectance anisotropy (defined as in Fig. 1), and for (b) the unpolarized reflectivity, calculated for Si(100) ( $2 \times 1$ ).

cides with that of a naive picture of the dimers considered as isolated  $\text{Si}_2$  molecules. This can be explained on the basis of the omission, in the TB approach, of the direct interaction between atoms belonging to adjacent dimers. In fact, the explanation of this apparently paradoxical sign of the reflection anisotropy can be found looking at the surface band structure:<sup>26</sup> the dispersion of the surface-localized  $\pi$  and  $\pi^*$  bands along the row direction (i.e., perpendicularly to the dimers) is comparable to the  $\pi$ - $\pi^*$  separation. This means that the interaction between adjacent dimers is about as large as the interaction between the  $p_z$  orbitals of the two atoms in a single dimer. Hence, the correct picture of these surfaces is that of interacting chains of dimers, oriented in the direction perpendicular to the dimers themselves, and separated by large valleys through which the dimers interact very weakly. Recently Gavrilenko and Pollack performed theoretical calculations both with the DFT-LDA and the TB schemes.<sup>16</sup> However, while their TB results agree with our calculations, their DFT-LDA spectra, which are obtained with some kind of “*ad hoc*” treatment of the self-energy effects, appear to

be at variance with both our results and the calculations of Ref. 3, and do not correctly describe the experimental spectra.

In Fig. 4(b) we compare the *unpolarized* reflectivity spectra obtained in our TB and LDA calculations, using the same geometry (buckling of 0.56 Å). In this case, our *ab initio* calculation of the SDR spectra basically agree with the TB results and with previously published data,<sup>1</sup> confirming that once averaged over the polarizations the spectra depend less critically on the theoretical scheme used. In particular, the occurrence of the (experimentally measured) first peak at about 1.4 eV as a consequence of dimer buckling, which was the main point of Ref. 1, is confirmed. In the case of unbuckled dimers, in fact, the first SDR peak occurs at 0.9 eV, where the first RAS structure in Fig. 1 occurs.

## V. CONCLUSIONS

We have carried out *ab initio* calculations of the optical properties of the Si(100) surface within DFT-LDA. For the first time this approach has been applied to the  $c(4 \times 2)$  clean surface and to the  $(1 \times 1)$  hydrogenated surface. Quite surprisingly, the optical properties of the  $c(4 \times 2)$  reconstructed surface are qualitatively different from those of the  $p(2 \times 2)$  phase on the low-frequency side. A qualitative understanding of RAS and SDR measurements is obtained. The structure appearing below 1 eV in the SDR spectrum, not well understood so far, is naturally explained in terms of the occurrence of  $c(4 \times 2)$  domains.

Our *ab initio* DFT-LDA calculations allow us to check the reliability of the TB approach. SDR TB spectra are in qualitative agreement with DFT-LDA spectra, while some discrepancy appears in the case of RAS spectra, which are more sensitive to the details of the local geometry and require more accurate calculations. The omission of second-neighbor interactions in the  $sp^3s^*$  scheme used in our and previous TB calculations is mostly responsible for this discrepancy. Calculations using a second-neighbors parametrization scheme should correct this shortcoming of the TB approach.

## ACKNOWLEDGMENTS

We are grateful to S. Goedecker for providing us an efficient code for fast Fourier transforms.<sup>35</sup> This work was supported in part by the European Community program “Human Capital and Mobility” (Contract No. ERB CHRX CT930337) and by the INFN Parallel Computing Initiative. Calculations were performed at CINECA (Interuniversity Consortium of the Northeastern Italy for Automatic Computing). B.S.M. thanks partial support of CONACyT-México (26651-E) and CNR-Italy through a collaboration program.

<sup>1</sup>A. Shkrebtii and R. Del Sole, Phys. Rev. Lett. **70**, 2645 (1993).

<sup>2</sup>F. Manghi, R. Del Sole, A. Selloni, and E. Molinari, Phys. Rev. B **41**, 9935 (1990).

<sup>3</sup>L. Kipp, D. K. Biegelsen, J. E. Northrup, L.-E. Swartz, and R. D. Bringans, Phys. Rev. Lett. **76**, 2810 (1996).

<sup>4</sup>O. Pulci, G. Onida, R. Del Sole, and A. Shkrebtii, Phys. Rev. B **58**, 1922 (1998).

<sup>5</sup>P. Hohenberg and W. Kohn, Phys. Rev. **136**, B864 (1964); W. Kohn and L. J. Sham, *ibid.* **140**, A1133 (1965).

<sup>6</sup>D.M. Ceperley and B.J. Alder, Phys. Rev. Lett. **45**, 566 (1980); J.P. Perdew and A. Zunger, Phys. Rev. B **23**, 5048 (1981).

<sup>7</sup>J.E. Northrup, Phys. Rev. B **47**, 10 032 (1993).

<sup>8</sup>L.S. Johansson, R.I.G. Uhrberg, P. Martensson, and G. W. Hansson, Phys. Rev. B **42**, 1305 (1990).

- <sup>9</sup>L.S. Johansson and B. Reihl, Surf. Sci. **269/270**, 810 (1992).
- <sup>10</sup>T. Tabata, T. Aruga, and Y. Murata, Surf. Sci. **179**, L63 (1987).
- <sup>11</sup>T. Yokoyama and K. Takayanagi, Phys. Rev. B **57**, R4226 (1997).
- <sup>12</sup>A. I. Shkrebtii, R. Di Felice, C.M. Bertoni, and R. Del Sole, Phys. Rev. B **51**, R11 201 (1995).
- <sup>13</sup>M. Kubots and Y. Murata, Phys. Rev. B **49**, 4810 (1994).
- <sup>14</sup>H. Shigekawa, K. Hata, K. Miyake, M. Ishida, and S. Ozawa, Phys. Rev. B **55**, 15 448 (1997).
- <sup>15</sup>C. Kress, A.I. Shkrebtii, and R. Del Sole, Surf. Sci. **377-379**, 398 (1997).
- <sup>16</sup>V. I. Gavrilenko and F. H. Pollak, Phys. Rev. B **58**, 12 964 (1998).
- <sup>17</sup>R. Shioda and J. van der Weide, Phys. Rev. B **57**, R6823 (1998).
- <sup>18</sup>S. G. Jaloviar, J.-L. Lin, F. Liu, V. Zielasek, L. McCaughan, and M. G. Lagally, Phys. Rev. Lett. **82**, 791 (1999).
- <sup>19</sup>R. Del Sol, in *Photonic Probes of Surfaces*, edited by P. Halevi (Elsevier, Amsterdam, 1995), p. 131, and references therein.
- <sup>20</sup>R. Del Sole and E. Fiorino, Phys. Rev. B **29**, 4631 (1984).
- <sup>21</sup>A.F. Starace, Phys. Rev. A **3**, 1242 (1977).
- <sup>22</sup>G. Bachelet, D.R. Hamann, and M. Schlüter, Phys. Rev. B **26**, 4199 (1982).
- <sup>23</sup>L. Kleinman and D.M. Bylander, Phys. Rev. Lett. **48**, 1425 (1982).
- <sup>24</sup>P. Kruger and J. Pollman, Phys. Rev. Lett. **74**, 1155 (1995).
- <sup>25</sup>R. Del Sole and R. Girlanda, Phys. Rev. B **48**, 11 789 (1993).
- <sup>26</sup>A. Ramstad, G. Brooks, and P.J. Kelly, Phys. Rev. B **51**, 14 504 (1995).
- <sup>27</sup>T. Yokoyama, M. Okamoto, and K. Takayanagi, Phys. Rev. Lett. **81**, 3423 (1998).
- <sup>28</sup>The experimental RAS data of Refs. 17 and 18 are similar. We quote in Fig. 2 those of Ref. 17 because they include the frequency range from 1 to 2 eV, which is especially interesting for surface-state transitions.
- <sup>29</sup>R.J. Cole, S. Tanaka, P. Gerber, J.R. Power, and T. Farrell, Phys. Rev. B **54**, 13 444 (1996).
- <sup>30</sup>T. Yasuda, L. Mantese, U. Rossow, and D.E. Aspnes, Phys. Rev. Lett. **74**, 3431 (1995).
- <sup>31</sup>Y.J. Chabal, S.B. Christman, E. E. Chaban, and M. T. Yin, J. Vac. Sci. Technol. A **1**, 1241 (1983).
- <sup>32</sup>P.E. Wierenga, A. van Silfhout, and M.J. Spaarnay, Surf. Sci. **99**, 59 (1980).
- <sup>33</sup>E.G. Keim, L. Wolterbeek, and A. Van Silfhout, Surf. Sci. **180**, 565 (1987).
- <sup>34</sup>H. Farrell, F. Stuck, J. Anderson, D. J. Frankel, G. J. Lapeyre, and M. Levinson, Phys. Rev. B **30**, 721 (1984).
- <sup>35</sup>S. Goedecker, Comput. Phys. Commun. **76**, 294 (1993); S. Goedecker, SIAM J. Sci. Comput. **18**, 1605 (1997).